Journal of Advanced Ceramics
2013, 2(1): 21–25
DOI: 10.1007/s40145-013-0036-2 ISSN 2226-4108

Research Article

Theoretical calculation and analysis of ZrO_2 spherical nanometer powders

Ying CHANG[a], Huihu WANG[b], Qinbiao ZHU[a], Ping LUO[b], Shijie DONG[b,*]

[a]*Department of Materials*, *School of Chemical and Environment Engineering*, *Hubei University of Technology*, *Wuhan 430068*, *China*
[b]*School of Mechanical Engineering*, *Hubei University of Technology*, *Wuhan 430068*, *China*

Received: October 09, 2012; Revised: December 22, 2012; Accepted: December 25, 2012

Abstract: ZrO_2 spherical nanometer powders containing 3.5 mol% Y_2O_3 have been prepared via the coupling route of water/oil (W/O) emulsion with dimethyl oxalate homogenous precipitation. ZrO_2 powders and their precursor powders have been characterized by XRD, TEM and SEM. According to the XRD result, phase volume fractions of powders were calculated by comparing the peaks' intensities of spectrum. Furthermore, phase crystal lattice constants were obtained using crystal interplanar spacing formula and Bragg equation. With these results, the theoretical density of powders was analyzed. Finally, powders' spherical degree was revealed via the method of comparison between theoretical density and actual density.

Keywords: spherical; zirconia nanometer powders; theoretical calculation; density

1 Introduction

ZrO_2 is widely applied in many advanced structural ceramics, high-temperature ceramics and electronic devices for its low thermal conductivity, high mechanical strength and relatively high thermal expansion coefficient [1–4]. It is well known that powder performance determines the final manufacture and performance of ceramic products. To obtain uniform microstructure with a low sintering temperature and high density, the particles of ceramic powders must be spherical with narrow size distribution [5–7]. Nanometer particles can further enhance the low-temperature sintering performance of ceramics and enable the ceramics to possess a smaller residual porosity and the grain size [8–11]. Therefore, the preparation of ZrO_2 spherical nanometer particles has been the research focus in recent years [12–16].

Different characterization methods, such as TEM and SEM have been applied to analyze the spherical degree of ZrO_2 powders. However, these methods are not very reasonable. For example, TEM photographs of spherical nanometer particles only indicate that they are spherical in the projection direction, but it may be inappropriate to think they are three-dimensional pellets. Therefore, it is more convincing and necessary to illustrate the spherical degree of powders by using the combination method of theoretical calculation and actual characterization.

The experiments in this paper adopted the emulsion system to synthesize ZrO_2 spherical nanometer particles, in which system cheap xylol was used as the oil phase, span-80 as the surfactant, and aqueous solution

* Corresponding author.
E-mail: dongsjsj@163.com

containing $Zr(NO_3)_4$, $Y(NO_3)_3$ and dimethyl oxalate as the water phase. During the water bath process, dimethyl oxalate hydrolysis was decomposed into precipitator, and the precipitates became spherical grains in the water droplets of emulsion. As a result, ZrO_2 (with 3.5 mol% Y_2O_3) nanometer powders with excellent dispersion, spherical shape and narrow particle size distribution can be prepared via the coupling route of water/oil (W/O) emulsion with dimethyl oxalate homogenous precipitation [17]. XRD, TEM and SEM patterns were carried out to analyze the microstructures of spherical ZrO_2 powders. The phase volume fractions, phase crystal lattice constants and the theoretical density of powders were calculated according to above characterization results. The powders' spherical degree was verified via the method of comparison between theoretical density and actual density.

2 Experiments

2.1 Experimental methods

At room temperature, $Zr(NO_3)_4{\cdot}2H_2O$ (AR) and $Y(NO_3)_3{\cdot}6H_2O$ (AR) were confected into 0.5 mol/L solution. Then the solution was added into the dimethyl oxalate containing surfactant span-80 with continuously stirring by a magnetic stirrer. After that, the mixed solution was dispersed supersonically for another 20 minutes. Then it was transferred to a water bath which was slowly heated to 90 ℃ and kept for 1 h. The mixed solution turned into white gels during this process, which were treated with method of azeotropic distillation to get distilled gels. The obtained distilled gels were filtered and washed with deionized water several times to remove the residual surfactants and oil phase. The deionized water in gels was eliminated through washing with ethyl-alcohol. Finally, the gels were dried at 80 ℃ in vacuum for 24 h and calcined at 600 ℃ for 1 h to produce crystalline ZrO_2 powders. The reaction principle was expressed as follows:

$$C_2O_4(CH_3)_2 + H_2O \rightarrow C_2O_4H_2 + CH_3OH$$

$$C_2O_4H_2 \rightarrow C_2O_4^{2-} + 2H^+$$

$$C_2O_4^{2-} + Zr^{4+} \rightarrow Zr(C_2O_4)_2$$

2.2 Characterization of powders

The XRD spectrums were carried out via internal standard method with an X-ray diffractometer (operating at 40 kV, 300 mA, using Cu Kα radiation, $\lambda = 0.154\,056$ nm). The particle morphologies were obtained by transmission electron microscopy (JEM-2100FS) and scanning electron microscopy (JSM-6300LV).

3 Results and discussion

3.1 The calculation of phase volume fractions

The X-ray spectrum of as-prepared nanometer powders is shown in Fig. 1. It can be seen that ZrO_2 powders are composed of the tetragonal phase and the cubic phase.

In the XRD spectrum, cubic and tetragonal phase diffraction peaks of ZrO_2 powders are very close to each other, and it is very difficult to distinguish them in peak position with strong diffraction intensity. Therefore, t (400) and c (400) diffraction peaks are often analyzed on the test [18]. The volume fractions of phase are calculated using the following equations (Eqs. (1) and (2)), where the terms I_t(004), I_t(400) and I_c(400) correspond to the intensities of the peaks (004), (400) of the tetragonal phase and (400) of the cubic phase. Footnotes t and c represent tetragonal phase and cubic phase, respectively. In addition, Fig. 2 shows

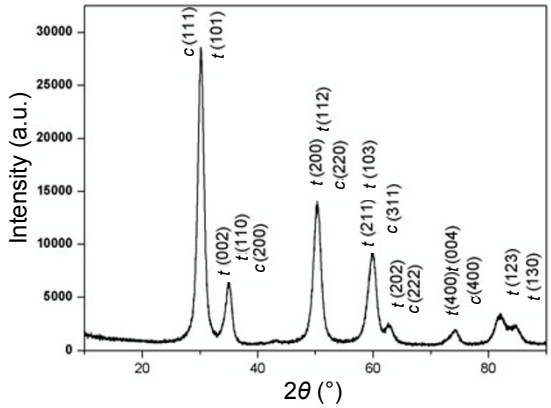

Fig. 1 X-ray spectrum of nanometer structured powders under 600 ℃ calcination temperature.

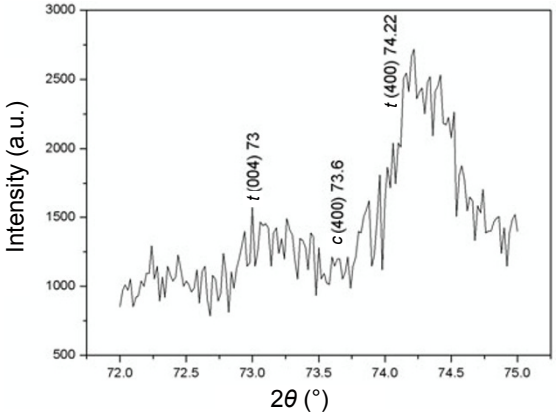

Fig. 2 X-ray spectrum of powders ($2\theta = 72°$–$75°$).

the enlarged X-ray spectrum ($2\theta = 72°–75°$) of powders, and Table 1 gives the (004) and (400) diffraction peak intensities of XRD spectrum.

Table 1 The (004) and (400) diffraction peak intensityes of XRD spectrum

Peak	Intensity (a.u.)
t (004)	1573.33
c (400)	1213.33
t (400)	2720.00

$$v_{at}(\text{mol\%}) = \frac{I_t}{I_c + I_t} = \frac{I_t(004) + I_t(400)}{I_c(400) + I_t(004) + I_t(400)} = \frac{1573.33 + 2720}{1213.33 + 1573.33 + 2720} = 0.78 \quad (1)$$

$$v_{ac}(\text{mol\%}) = \frac{I_c}{I_c + I_t} = \frac{I_c(400)}{I_c(400) + I_t(004) + I_t(400)} = \frac{1213.33}{1213.33 + 1573.33 + 2720} = 0.22 \quad (2)$$

As a result, phase volume fractions of powders were calculated according to Eqs. (1) and (2). It consists of 0.78 mol% tetragonal phase and 0.22 mol% cubic phase.

3.2 Crystal lattice constant calculation of powders

Crystal lattice constants have been calculated with the crystal face spacing formula and Bragg equation according to crystal faces of the XRD diffraction spectrum (Fig. 2). Crystal lattice constants include the cubic phase lattice constant a_c and the tetragonal phase lattice constant a_t.

Tetragonal phase crystal interplanar spacing can be expressed by

$$d = a_t / \sqrt{h^2 + k^2 + l^2 / (c_t / a_t)^2} \quad (3)$$

The face spacing d between the (h00) crystal faces is as follows:

$$d_{(h00)} = \frac{a_t}{h} \quad (4)$$

According to Bragg equation (λ=0.154 056 nm):

$$2d\sin\theta = \lambda \quad (5)$$

$$2d_{(h00)}\sin\theta_{(h00)} = \lambda \quad (6)$$

$$2\frac{a_t}{h}\sin\theta_{(h00)} = \lambda \quad (7)$$

The tetragonal phase crystal lattice constant a_t has been calculated with above equations and the tetragonal phase crystal face (400) diffraction angle of powders, and the value is 0.510 67 nm.

Similarly, the cubic phase crystal interplanar spacing formula is as follows:

$$d = \frac{a_c}{\sqrt{h^2 + k^2 + l^2}} \quad (8)$$

According to Bragg equation:

$$\frac{2a_c\sin\theta}{\sqrt{h^2 + k^2 + l^2}} = \lambda \quad (9)$$

The cubic phase lattice constant a_c of powders can be calculated according to the cubic phase crystal face (400) diffraction angle, and the value is 0.514 357 nm.

Therefore, the average crystal lattice constant of powders can be expressed with the following formula:

$$a = a_t \cdot v_{at} + a_c \cdot v_{ac} = 0.51067 \times 0.78 + 0.514357 \times 0.22 = 0.51148 \text{ nm} \quad (10)$$

where v_{at} and v_{ac} represent the tetragonal phase volume fraction and the cubic phase volume fraction respectively.

In addition, Ingel and Lewis have deduced the experience formula for calculating t-ZrO_2 or c-ZrO_2 lattice constant a (unit: Å) according to the sphere packing model [19]:

$$a = 23.094\left[0.221 + \frac{\sum_{i=1}^{n} P_i M_i (R_i - 0.081)}{100 + \sum_{i=1}^{n} M_i (P_i - 1)}\right] = 23.094\left[0.221 + \frac{2 \times 3.5(0.090 - 0.081)}{100 + 3.5(2-1)}\right] = 5.1178 \quad (11)$$

where P_i represents the metal element ion number of stabilizer M_xO_y, M_i represents molar percentage of stabilizer M_xO_y, R_i represents ionic radius of metal M (such as $R_{Zr} = 0.081$ nm, $R_Y = 0.090$ nm).

Therefore, the value of crystal lattice constant is 0.511 78 nm according to the calculation result of Eq. (11). It is very close to 0.511 48 nm.

3.3 Calculation of powder theoretical density

The theoretical density ρ_0 (unit: g/cm^2) of powders can be calculated with the following formula according to the crystal lattice constant values [18]:

$$\rho_0 = \frac{6.6412}{a^3}\left\{123.22 + \frac{\sum_{i=1}^{n} P_i M_i [(A_i - 91.22) + (P_{oi}/P_i - 2) \times 16]}{100 + \sum_{i=1}^{n} M_i (P_i - 1)}\right\} = \frac{6.6412}{5.1148^3}\left\{123.22 + \frac{2 \times 3.5[(88.91 - 91.22) + (3/2 - 2) \times 16]}{100 + 3.5(2-1)}\right\} = 6.081 \quad (12)$$

where P_i represents the metal element ion number of stabilizer M_xO_y, M_i represents molar percentage of stabilizer M_xO_y, A_i represents atomic weight of metal element M of stabilizer M_xO_y, P_{oi} represents the oxide-ion number of stabilizer M_xO_y, a is the average crystal lattice constant of powders.

Therefore, the theoretical density ρ_0 of powders is 6.081 g/cm^2 according to the calculation result of Eq. (12). It is very close to the density 6.111 g/cm^2 which comes from the formula $d=6/(\rho S_{BET})$ [20], where d is the particle size, ρ is the density of the powers, S_{BET} is the BET surface area. The tenable condition of this formula is that pellets are assumed as sphere. It can also prove that the prepared powders possess excellent spherical shape.

3.4 Microscopic morphology of powders

TEM and SEM images of powders are respectively shown in Figs. 3(a) and 3(b). It can be seen from Fig. 3(a) that the powders possess excellent spherical shape and dispersion degree. At the same time, the sintering necks of powders have already appeared at 600 ℃, demonstrating that the powders' surface is very active. In addition, it can be seen from Fig. 3(b) that the reunion or agglomeration of powders is loose. The particle size distribution is extremely uniform, and the reunion particle possesses spherical or nearly spherical appearance.

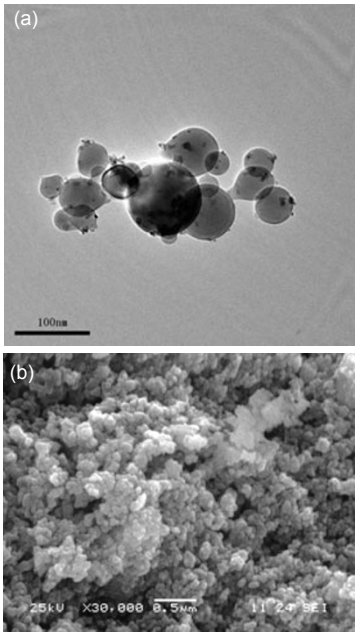

Fig. 3 Images of the ZrO_2 powders obtained by means of the transmission electron microscopy and scanning electron microscopy.

4 Conclusions

ZrO_2 nanometer powders containing 3.5 mol% Y_2O_3 have been prepared via the coupling route of W/O emulsion with dimethyl oxalate homogenous precipitation. The powders possess spherical shape, excellent dispersing property and fine size distribution. The phase volume fractions of powders have been calculated, and the result is 0.78 mol% tetragonal phase and 0.22 mol% cubic phase. Furthermore, the phase crystal lattice constants have been calculated, and the results are as follows: $a_c = 0.514\,357$ nm, $a_t = 0.510\,67$ nm.

The theoretical density ρ_0 of powders has been calculated as being 6.081 g/cm^2, which is very close to the actual density, and the result shows that the prepared powders possess excellent spherical shape.

Acknowledgements

The authors acknowledge the support of the National Natural Science Foundation of China (Grant Nos. 51004046 and 51075129), the State Key Development Program for Basic Research of China (Project No. 2010CB635107), and the National Natural Science Foundation of Hubei Province of China (Project No. 2010CDB05806).

References

[1] Malzbender J. The use of theories to determine mechanical and thermal stresses in monolithic, coated and multilayered materials with stress-dependent elastic modulus or gradient in elastic modulus exemplified for thermal barrier coatings. *Surf Coat Technol* 2004, **186**: 416–422.

[2] Huang YY, Chen JT, Ni JF, *et al*. A modified ZrO_2-coating process to improve electrochemical performance of $Li(Ni_{1/3}Co_{1/3}Mn_{1/3})O_2$. *J Power Sources* 2009, **188**: 538–545.

[3] Yao ZP, Jiang YL, Jiang ZH, *et al*. Preparation and structure of ceramic coatings containing zirconium oxide on Ti alloy by plasma electrolytic oxidation. *J Mater Process Tech* 2008, **205**: 303–307.

[4] Suzana J, Willy H, Danny H, *et al*. Characterisation of ZrO_2 layers deposited on Al_2O_3 coating. *Wear* 2009, **266**: 417–423.
[5] Winnubst AJA, Groot Zevert WFM, Theunissen GSAM, *et al*. Microstructure characteristics of ultra-fine ZrO_2 Y_2O_3 ceramic powders. *Mat Sci Eng A* 1989, **109**: 215–219.
[6] Lange FF. Powder processing science and technology for increased reliability. *J Am Ceram Soc* 1989, **72**: 3–15.
[7] Rhodes WH. Agglomerate and particle size effects on sintering yttria-stabilized zirconia. *J Am Ceram Soc* 1981, **64**: 19–22.
[8] Van De Graaf MACG, Ter Maat JHH, Burggraaf AJ. Microstructure and sintering kinetics of highly reactive ZrO_2–Y_2O_3 ceramics. *J Mater Sci* 1985, **20**: 1407–1418.
[9] Theunissen GSAM, Winnubst AJA, Burggraaf AJ. Sintering kinetics and microstructure development of nanoscale Y–TZP ceramics. *J Eur Ceram Soc* 1993, **11**: 315–324.
[10] Durán P, Villegas M, Lapel F, *et al*. Low temperature fully densified nanostructured Y TZP ceramics. *J Mater Sci Lett* 1996, **15**: 741–744.
[11] Lawson S. Environmental degradation of zirconia ceramics. *J Eur Ceram Soc* 1995, **15**: 485–502.
[12] Lee MH, Tai CY, Lu CH. Synthesis of spherical zirconia by precipitation between two water/oil emulsions. *J Eur Ceram Soc* 1999, **19**: 2593–2603.
[13] Joo J, Yu T, Kim YW, *et al*. Multigran scale synthesis and characterization of monodisperse tetragonal zirconia nanocrystal. *J Am Chem Soc* 2003, **125**: 6553–6557.
[14] Chang Y, Li XB. Preparation of ZrO_2 spherical nanometer powders via emulsion processing route. *Trans Nonferrous Met Soc China* 2006, **16**: 332–336.
[15] Xia B, Duan LY, Xie YC. ZrO_2 nanopowders prepared by low-temperature vapor-phase hydrolysis. *J Am Ceram Soc* 2000, **83**: 1077–1080.
[16] Wang XQ, Wang M, Zhu XY, *et al*. Preparation of ZrO_2 spherical nanoparticles used for photonic crystal. *Adv Mat Res* 2012, **412**: 57–60.
[17] Chang Y, Li XB, Meng ZQ, *et al*. Preparation of ZrO_2 (Y_2O_3) spherical nanometer powders via coupling route of water–oil emulsion with homogenous precipitation. *Chin J Nonferrous Met* 2006, **16**: 73–78 (in Chinese).
[18] Shen SM. The preparation and performance study of nanofilm and nanocrystalline material. Master Thesis. Lanzhou: Lanzhou University, 2001 (in Chinese).
[19] Ingel RP, Lewis III D. Lattice parameters and density for Y_2O_3-stabilized ZrO_2. *J Am Ceram Soc* 1986, **69**: 325–332.
[20] Kavan L, Grätzel M. Facile synthesis of nanocrsytalline $Li_4Ti_5O_{12}$ (spinel) exhibiting fast Li insertion. *Electrochem Solid-State Lett* 2002, **5**: A39–A42.